e-J. Surf. Sci. Nanotech. Vol. 4 (2006) 410-413 Conference -ALC05-

Single layer hexagonal boron nitride films on Ni(110) *

Thomas Greber,† Louis Brandenberger, Martina Corso, Anna Tamai, and Jürg Osterwalder
Physik Institut der Universität Zürich, Winterthurersrasse 190, CH-8057 Zürich, Switzerland
(Received 28 November 2005; Accepted 5 April 2006; Published 19 April 2006)

Hexagonal boron nitride was grown on nickel (110) by chemical vapor deposition of borazine. The *h*-BN layers on Ni(110) were investigated by low energy electron diffraction (LEED) and angular resolved photoemission (ARUPS). LEED shows a (1×6) and a (7×5) super structure. ARUPS from the σ bands of *h*-BN indicates single layer *h*-BN, but two different orientations of the *h*-BN Brillouin zones with a relative weight of 6:1. This is in line with lock in energy arguments, which consider coincidence lattices between nickel top atoms and nitrogen atoms. [DOI:10.1380/ejssnt.2006.410]

Keywords: hexagonal boron nitride; ferromagnetic samples

I. INTRODUCTION

Monolayers of hexagonal boron nitride on transition metals form a class of interface systems with properties of a metal insulator interface. They are thermally stable, chemically inert and form well defined tunneling barriers for electrons. This is particularly interesting if the electronic time scale for hopping shall be increased in order to get a better coupling to slower degrees of freedom such as molecular rotations [1].

The investigation of *h*-BN layers on transition metals has a long standing history. Paffett et al. first used borazine $(HBNH)_3$ as a precursor to form *h*-BN layers on Pt(111) and Ru(001) transition metal surfaces, where the lattice mismatch causes large coincidence lattice unit cells [2]. Close inspection of such a 12×12 coincidence lattice on Rh(111) showed a 'nanomesh', a surprisingly complicated double layer *h*-BN structure with about 400 atoms in the unit cell [3]. The lattice constants of nickel and cobalt match well with that of *h*-BN layers, in particular the substrate lattice constant is slightly smaller than that of *h*-BN. Nagashima et al. first investigated *h*-BN/Ni(111) [4]. On Ni(111) a (1×1), single domain structure forms, which is well characterized by experiments [5, 6] and theory [7]. It has to be emphasized that the quality of *h*-BN/Ni(111) is very sensitive to the preparation history of the sample. It was e.g. seen that slightly different preparation procedures could lead to a (1×1) domain [7, 8], which is rotated by 180° with respect to that of Gamou et al. [5].

h-BN/Ni is particularly interesting in view of investigations on spintronic interfaces, since nickel is ferromagnetic [9]. It is also desirable to grow perfect layers of *h*-BN on Ni surfaces with other orientations than the close packed (111) surface. This has been realized on Ni(100), without using borazine as a precursor, where Desrosiers et al. found a (1×7) superstructure which is consistent with a monolayer of strained *h*-BN [10]. On vicinal Ni surfaces borazine exposure at 1000 K results in strong facetting of the Ni surface [11, 12]. In view of spin polarized electron spectroscopy experiments Ni(110) is the substrate of choice since we find, in contrast to Ni(111) and Ni(100), ⟨111⟩ easy magnetisation axes in the surface plane [13]. Here we report on the preparation of single layer *h*-BN on Ni(110), where we find a closed layer, though with several superstructures.

II. EXPERIMENTAL

The experiments were performed in a modified VG ESCALAB 220 [14] on a Ni(110) single crystal (13×6.5×3 mm) (MatecK), with crystal orientations and yoke cut as shown in Fig. 1. The coil allows heating and/or magnetisation along the $[\bar{1}11]$ and $[1\bar{1}\bar{1}]$ direction, respectively. The sample was cleaned with standard Ar sputtering/annealing and O_2 titration cycles. The *h*-BN films were then prepared following the receipe of Nagashima et al. [15], where the surface is kept at 1000 K and exposed to 70 Langmuir $(40 \cdot 10^{-6}$ Torr s) of borazine.

III. RESULTS AND DISCUSSION

In Fig. 2 the He Iα excited normal emission spectrum are shown for *h*-BN/Ni(110). As on *h*-BN/Ni(111) [9, 16]

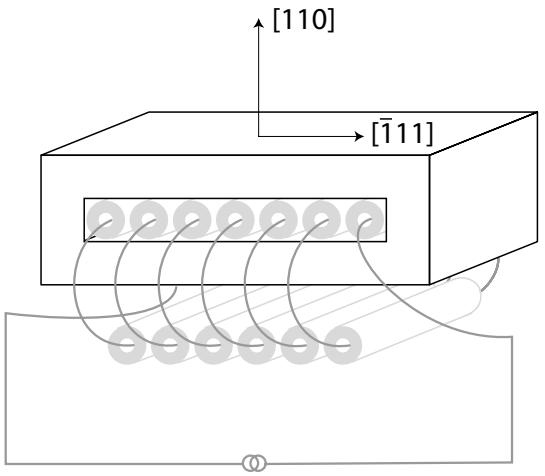

FIG. 1: Geometry of the Ni(110) sample (13×6.5×3 mm). The yoke is cut from a single crystal and allows preferential magnetisation along the $[\bar{1}11]$ easy axis. The coil is used for magnetisation and/or heating.

*This paper was presented at 5th International Symposium on Atomic Level Characterizations for New Materials and Devices (ALC05), Hawaii, USA, 4-9 December, 2005.

†Corresponding author: greber@physik.unizh.ch

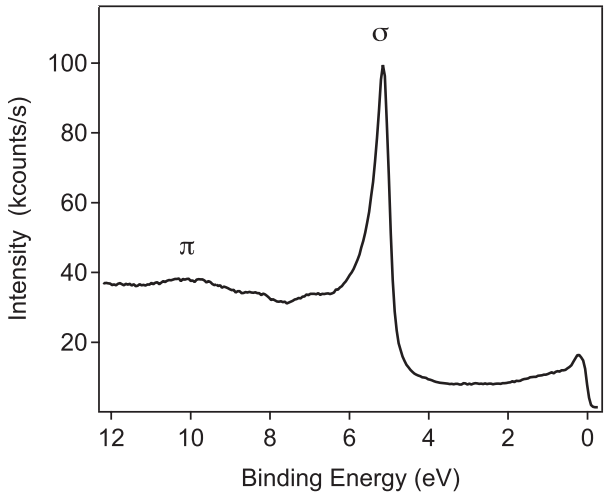

FIG. 2: He I α normal emission UP-spectra for h-BN/Ni(110). Along $\bar{\Gamma}$ the h-BN σ_1 and σ_2 bands were degenerate at a binding energy of 5.14 eV, the binding energy of the π band is 10.2 eV, and the work function is 3.8 eV.

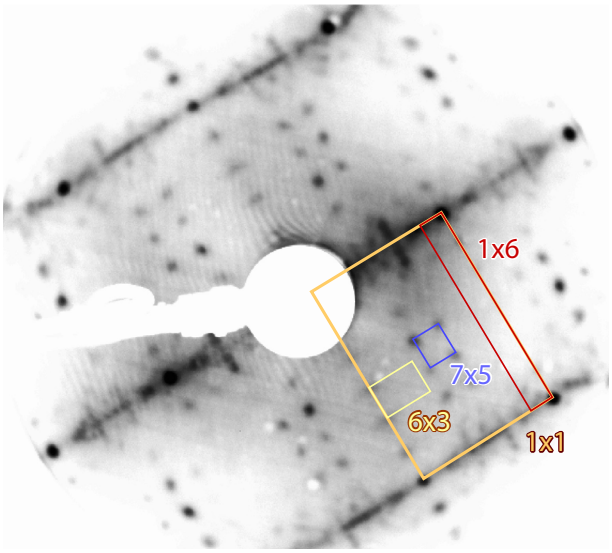

FIG. 3: Low energy electron diffraction (LEED) pattern (E_{kin} = 90.5 eV) from 1 monolayer h-BN on Ni(110). The unit cells as discussed in the text were marked.

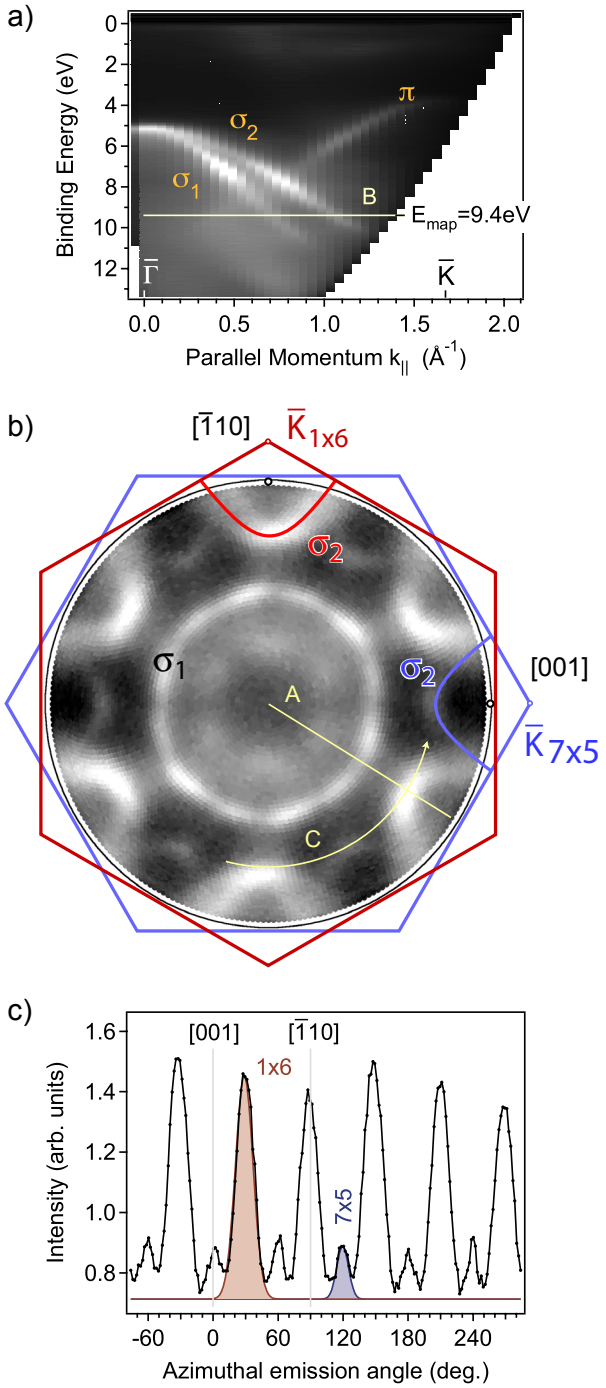

FIG. 4: Angular resolved He Iα photoelectron spectroscopy (ARUPS) data for h-BN/Ni(110). White is high intensity. a) Dispersion plot along the azimuth labeled A in b). Clearly, the dispersion of the σ-bands and the π-band correspond to the $\bar{\Gamma}\bar{K}$ direction in h-BN layers [7]. The cut B at $E_{\rm map}$ is the constant energy at which the map in b) has been measured. b) k-space map in $k_{||}$ projection. Two matching h-BN Brillouin zones with label (1×6) and (7×5) were marked. The polar cut A, shown in a) and the azimuthal cut C, shown in c) were displayed as well. No 6-fold averaging has been performed. c) Azimuthal cut across the σ_2 resonances at a polar angle $\theta = 47°$. The shaded Gaussians are a weight for the two different h-BN orientations.

one sharp σ band is visible. In contrast to h-BN/Rh(111), where a double layer is found [3], this indicates one closed layer of hexagonal boron nitride which lies parallel to the surface. The σ band binding energy at $\bar{\Gamma}$ is 5.14 eV, compared to 5.3 eV on Ni(111) [7]. Scanning tunneling microscopy shows a variety of different h-BN overlayer structures as it was also found for h-BN/Pd(110) [17]. This polymorphism is reflected in the low energy electron diffraction (LEED) patterns, which indicate several h-BN superstructures. Here we discuss the (1×6) and the (7×5) super structure. For the (6×3) structure we find no consistent overlayer model. The (1×6) and the (7×5) structures may be analyzed in a rigid lattice model (see Fig. 5). From Ni(111) it is known that h-BN fits almost perfectly. The lattice mismatch as defined by Zangwill $M = (a_f - a_s)/a_s$ is, with a h-BN film lattice constant a_f of a_{hBN}=2.504 Å and a Ni substrate lattice constant a_s of $a_{Ni(111)}$ = 2.492 Å, positive and +0.5% only. This mismatch is compensated with corrugation and produces

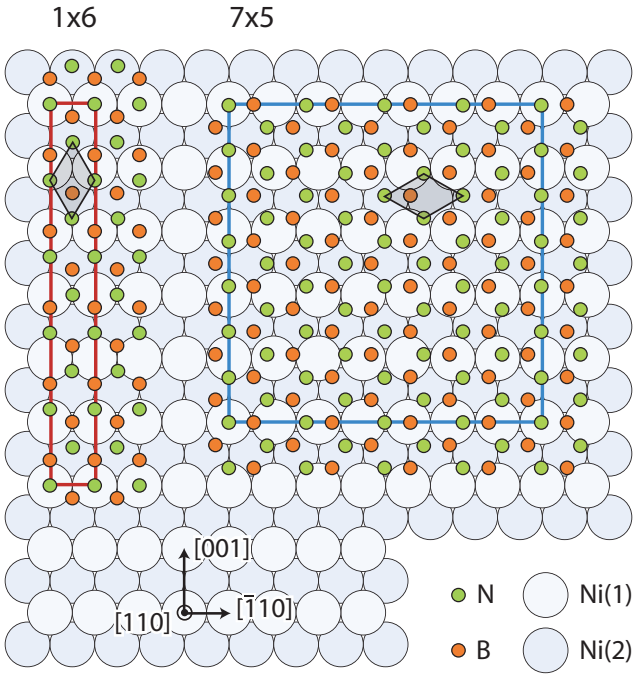

FIG. 5: Structure model for the h-BN/Ni(110) (1×6) unit cell with 10 BN pairs and the h-BN/Ni(110) (7×5) unit cell with 56 BN pairs. Note the different h-BN unit cell orientation. The corresponding h-BN mirror domains were equally probable, but not shown. Ni(1) are the row atoms in the Ni(110) surface.

perfect h-BN overlayers on Ni(111).

For the (1×6) structure on Ni(110) with one substrate lattice unit along the close packed $[\bar{1}10]$ rows and 6 substrate lattice units along [001] we get along $[\bar{1}10]$ a misfit $M^{\bar{1}10}_{1\times6} = +0.5\%$ and with $a_f = 5\sqrt{3}\ a_{hBN}$ and $a_s = 6\sqrt{2}\ a_{Ni(111)}$ $M^{001}_{1\times6} = +2.6\%$. The relatively large mismatch of +2.6% may be compensated by corrugation, which is also favored by the natural row structure of Ni(110). This structure has an orientation of the nitrogen triangles in the h-BN unit cell pointing along [001].

For the (7×5) structure on Ni(110) with 7 substrate unit cells along the close packed $[\bar{1}10]$ rows and 5 substrate lattice units along [001] we get $M^{\bar{1}10}_{7\times5} = -0.6\%$ and $M^{001}_{7\times5} = -0.5\%$. These negative mismatches may not be compensated by corrugation and will strain the system. Note: here the orientation of the nitrogen triangles is rotated by 90° with respect to the (1×6) structure i.e. along $[\bar{1}10]$.

From lock in energy arguments, without considering elastic energy costs, we expect the smaller (1×6) unit cell to dominate the (7×5) since there, the coincidence density, which is inversely proportional to the real space area of the super cell, is higher. It is likely that the coincidence leading to bonding is nitrogen on top of Ni atoms. This is justified by the proposed lone pair bonding of the nitrogen atoms [2] and the corresponding analogy to ammonia (NH_3), where the molecules tend to bind on top on Ni(111) [18], Ni(100) [19], and Ni(110) [20]. Together with the known N on top bonding of h-BN/Ni(111) [5, 7, 21] it is conjectured that this is also the case for Ni(100) and Ni(110).

We can access the branching into (1×6) and (7×5) structures by angular resolved ultra violet photoelectron spectroscopy (ARUPS). The h-BN overlayer in the two supercells has not the same azimuthal orientation i.e. the h-BN $\bar{\Gamma}\bar{\mathrm{K}}$ orientations of (1×6) and (7×5) are rotated by 90°. In the case of (1×6), $\bar{\Gamma}\bar{\mathrm{K}}_{1\times6}$ is parallel to $[\bar{1}10]$ and in the case of (7×5), $\bar{\Gamma}\bar{\mathrm{K}}_{7\times5}$ is parallel to [001]. Fig. 4 a) shows the dispersion of h-BN/Ni(110) along a $\bar{\Gamma}\bar{\mathrm{K}}_{1\times6}$ azimuth. Clearly, two σ bands, σ_1 and σ_2, and the π band of h-BN are resolved. Comparison with theory confirms this cut to show h-BN bands along $\bar{\Gamma}\bar{\mathrm{K}}$ [7]. We therefore choose a photoelectron energy (E_{map}=9.4 eV binding energy), where the h-BN σ_2 band produces a strong intensity on $\bar{\Gamma}\bar{\mathrm{K}}$, but not along $\bar{\Gamma}\bar{\mathrm{M}}$. In Fig. 4 b) 6 strong σ_2 resonances indicate the orientation of the h-BN domains that are favored. It coincides with $[\bar{1}10]$ and thus demonstrates the $\bar{\Gamma}\bar{\mathrm{K}}_{1\times6}$ h-BN orientation to dominate over the $\bar{\Gamma}\bar{\mathrm{K}}_{7\times5}$ orientation, which is visible as a weak replica of the main features and rotated by 90° with respect to $\bar{\Gamma}\bar{\mathrm{K}}_{1\times6}$. The replica occur within 0.5° at the same polar emission angle, and thus rule out a strong energy shift between the σ_2 bands of the two different structures. In Fig 4c) we see a cut at a polar emission angle of 47° across the data in Fig. 4b). From this, and assuming the same photoemission cross section for the two h-BN orientations we derive an area ratio between $\bar{\Gamma}\bar{\mathrm{K}}_{1\times6}$ and $\bar{\Gamma}\bar{\mathrm{K}}_{7\times5}$ of α=6.3:1, which is close to the Ni/N coincidence density ratio of $n_{1\times6} : n_{7\times5} = \frac{1}{10} : \frac{1}{56}$. In the azimuthal cuts of Fig. 4c) we find further information on the structure: The full width at half maximum of the $\sigma_2(7\times5)$ resonance is 13° compared to 19° for $\sigma_2(1\times6)$ which is consistent with the expectation of 'absence' of corrugation, i.e. 'perfect' flatness of the (7×5) structure. Fig. 5 shows the two models for the (1×6) and the (7×5) structures of h-BN on Ni(110) that base on LEED, and ARUPS data and the assumption of a nitrogen lock in on top of Ni atoms.

IV. CONCLUSION

In conlcusion, we observe single layers h-BN on Ni(110). Two overstructures with different weight were identified. The more abundant (1×6) and the (7×5) superstructures were close to coincidence lattices of the rectangular substrate and the hexagonal overlayer. Photoemission from the σ_2 band of h-BN clearly indicates the orientations of the hexagonal unit cells, which were rotated by 90° with respect to each other. This makes h-BN on Ni(110) a promising substrate for the study of spin related coupling at a metal insulator interface.

Acknowledgments

This study is supported by the Swiss National Science Foundation (SNF).

[1] M. Muntwiler, W. Auwärter, A.P. Seitsonen, J. Osterwalder, and T. Greber, Phys. Rev. B, **71**, 241401 (2005).

[2] M.T. Paffett, R.J. Simonson, P. Papin, and R.T. Paine,

Surf. Sci. **232**, 286 (1990).
[3] M. Corso, W. Auwärter, M. Muntwiler, A. Tamai, T. Greber, and J. Osterwalder, Science, **303**, 217 (2004).
[4] A. Nagashima, N. Tejima, Y. Gamou, T. Kawai, and C. Oshima, Phys. Rev. Lett., **75**, 3918 (1995).
[5] Y. Gamou, M. Terai, A. Nagashima, and C. Oshima, Sci. Rep. RITU **A44**, 211 (1997).
[6] W. Auwärter, T.J. Kreutz, T. Greber, and J. Osterwalder, Surf. Sci. **429**, 229 (1999).
[7] G.B. Grad, P. Blaha, K. Schwarz, W. Auwärter, and T. Greber, Phys. Rev. B **68**, 085404 (2003).
[8] W. Auwärter, M. Muntwiler, J. Osterwalder, and T. Greber, Surf. Sci. **545**, L735 (2003).
[9] T. Greber, W. Auwärter, M. Hoesch, G. Grad, P. Blaha, and J. Osterwalder Surf. Rev. Lett. **9**, 1243 (2002).
[10] R. M. Desrosiers, D.W. Greve, and A.J. Gellman, Surf. Sci. **382**, 35 (1997).
[11] E. Rokuta, Y. Hasegawa, A. Itoh, K. Yamashita, T. Tanaka, S. Otani, and C. Oshima, Surf. Sci. **427-428**, 97 (1999).
[12] M. Muntwiler, Thesis Universität Zürich (2004).
[13] M. Donath, Surf. Sci. Rep. **20**, 251 (1994).
[14] T. Greber, O. Raetzo, T. J. Kreutz, P. Schwaller, W. Deichmann, E. Wetli, and J. Osterwalder, Rev. Sci. Instrum. **68**, 4549 (1997).
[15] A. Nagashima, N. Tejima, Y. Gamou, T. Kawai, and C. Oshima, Phys. Rev. B **51**, 4606 (1995).
[16] T. Greber, W. Auwärter, G. Grad, P. Blaha, and J. Osterwalder: Proceedings of the Conference on Atomic Level Characterization (ALC01), Nara, Japan, (Nara-Ken New Public Hall 2002), 235.
[17] M. Corso, T. Greber, and J. Osterwalder, Surf. Sci. **577**, L78 (2005).
[18] A. Chattopadhyay, H. Yang, and J.L. Whitten, J. Chem. Phys. **94**, 6379 (1990).
[19] Y. Zheng, E. Moler, E. Hudson, Z. Hussain, and D.A. Shirley, Phys. Rev. B, **48**, 4760 (1993).
[20] H.E. Dastoor, P. Gardner, and D.A. King, Surf. Sci. **289**, 279 (1993).
[21] M. Muntwiler, W. Auwärter, F. Baumberger, M. Hoesch, T. Greber, and J. Osterwalder, Surf. Sci. **472**, 125 (2001).